International Journal of Applied Earth Observation and Geoinformation 46 (2016) 84–93

Contents lists available at ScienceDirect

International Journal of Applied Earth Observation and Geoinformation

journal homepage: www.elsevier.com/locate/jag

Modeling net primary productivity of terrestrial ecosystems in the semi-arid climate of the Mongolian Plateau using LSWI-based CASA ecosystem model

Gang Bao[a,b], Yuhai Bao[a,*], Zhihao Qin[c], Xiaoping Xin[c], Yulong Bao[a,b], Sainbuyin Bayarsaikan[d], Yi Zhou[e], Bilegtmandakh Chuntai[f]

[a] Inner Mongolia Key Laboratory of Remote Sensing and Geographic Information Systems, Inner Mongolia Normal University, Hohhot 010022, China
[b] College of Geographical Science, Inner Mongolia Normal University, Hohhot 010022, China
[c] Institute of Agro-Resources and Regional Planning, Chinese Academy of Agricultural Sciences, Beijing 100081, China
[d] Institute of Geography, Mongolian Academy of Science, Ulaanbaatar 14192, Mongolia
[e] School of Geography, Shanxi Normal University, Linfen 041000, China
[f] Department of Geography, Khovd University, Khovd, 84140, Mongolia

ARTICLE INFO

Article history:
Received 12 February 2015
Received in revised form
30 November 2015
Accepted 1 December 2015

Keywords:
Net primary productivity
Land-surface water index
CASA model
Mongolian Plateau
(semi-) Arid climate

ABSTRACT

Since the estimate of moisture stress coefficients (MSC) in the current Carnegie-Ames-Stanford-Approach (CASA) model still requires considerable inputs from ground meteorological data and many soil parameters, here we present a modified CASA model by introducing the land-surface water index (LSWI) and scaled precipitation to model the vegetation net primary productivity (NPP) in the arid and semiarid climate of the Mongolian Plateau. The field-observed NPP data and a previously proposed model (the Yu-CASA model) were used to evaluate the performance of our LSWI-based CASA model. The results show that the NPP predicted by both the LSWI-based CASA model and the Yu-CASA model showed good agreement with the observed NPP in the grassland ecosystems in the study area, with coefficients of determination of 0.717 and 0.714, respectively. The LSWI-based CASA model also performed comparably with the Yu-CASA model at both biome and per-pixel scales when keeping other inputs unchanged, with a difference of approximately 16 g C in the growing-season total NPP and an average value of 2.3 g C bias for each month. This indicates that, unlike an earlier method that estimated MSC based entirely on climatic variables or a soil moisture model, the method proposed here simplifies the model structure, reduces the need for ground measurements, and can provide results comparable with those from earlier models. The LSWI-based CASA model is potentially an alternative method for modelling NPP for a wide range of vegetation types in the Mongolian Plateau.

1. Introduction

Vegetation net primary productivity (NPP) is defined as the net accumulation of organic matter through photosynthesis by green plants per unit of time and space and represents the net primary source of food energy for Earth's living entities, including human beings (Yu et al., 2009a). It is a key component of the terrestrial carbon cycle (Piao et al., 2005) and serves as a sensitive indicator of ecosystem performance at both local and global scales (Lobell et al., 2002). Quantitative estimates of NPP at regional to global scales are therefore significant for understanding changes in ecosystem structure and function, predicting terrestrial carbon cycle trends (Field et al., 1995; Nemani et al., 2003; Yu et al., 2009a), determining sustainable use of natural resources, and making policy decisions (Mu et al., 2013a,b).

Remote sensing is currently regarded as a powerful and unique tool for characterizing vegetation structure both globally and reproducibly and has also played an increasing role in estimating ecosystem NPP (Hicke et al., 2002; Running et al., 2000; Zhao and Running, 2010). Numerous RS-based models for estimating NPP, such as the Carnegie-Ames-Stanford-Approach (CASA) model (Potter et al., 1993), the MOD-Sim-Cycle model (Hazarika et al., 2005), the GLO-PEM model (Prince, 1991), and the Biome-BGC model (Running et al., 2000), have been developed in recent decades to study the dynamics of vegetation productivity and its responses to climate change and anthropogenic activities at

* Corresponding author.
E-mail address: baoyuhai@imnu.edu.cn (Y. Bao).

http://dx.doi.org/10.1016/j.jag.2015.12.001
0303-2434/

scales ranging from local to global. However, several recent studies have highlighted that all these models for estimating NPP globally have a number of uncertainties and systematic errors when implemented in certain specific ecoregions (Fensholt et al., 2006; Yu et al., 2009b; Zhao et al., 2005, 2006), although their results are excellent at the global scale (Nemani et al., 2003; Potter et al., 1993). For example, the MODIS NPP products (MOD17A3), which are the first regular and near-real-time vegetation primary productivity data sets modeled by the Biome-BGC model at 1 km resolution, contain considerable errors in certain small regions (Zhao et al., 2005), particularly in some regions with arid and semi-arid climate (Fensholt et al., 2006) and tropical regions (Zhao et al., 2006). These errors arise because of the coarse and inconsistent spatial resolution of the meteorological reanalysis data (not the observed data) ($1.00° \times 1.25°$) compared with the MODIS pixels ($1\,km \times 1\,km$) (Sims et al., 2008). These reanalysis data were used as a key input for MODIS NPP modeling (Sims et al., 2008; Zhao et al., 2005). Another reason for the uncertainties of the MODIS NPP products in certain small regions may be that global-scale studies may neglect small-scale heterogeneity to some extent if local heterogeneity did not have a decisive effect on the whole (Bao et al., 2015). Furthermore, the MODIS NPP products provide only annual NPP (annual summations) (Running et al., 2000; Zhao et al., 2005), making it impossible to perform analysis at finer temporal scales (such as seasonal, monthly, or shorter timescales).

Therefore, it is imperative to improve or adjust these models, which were developed at a global scale, to adapt to different ecosystems in specific ecoregions as well as finer temporal scales by introducing available local information (Yu et al., 2009b) or other remote-sensing information (Sims et al., 2006b). In particular, models that are based entirely on remote-sensing data and can therefore produce truly continuous output at the same spatial resolution as satellite imagery are increasingly becoming a major focus of ecological modelers (Sims et al., 2006b; Wu et al., 2010a,b). Among the models that estimate NPP globally, the CASA ecosystem model, also called the light-use efficiency (LUE) model, is one of the most widely used models which adequately addresses NPP spatial and temporal dynamics at regional to global scales (Field et al., 1995; Mu et al., 2013b; Piao et al., 2005; Potter et al., 1993). Its success at the global scale is primarily due to its incorporation of per-pixel remote-sensing observations into the model and the relative simplicity of its algorithm (Mu et al., 2013b; Yu et al., 2009b). The fundamental concept of NPP for a given location x and time t in the CASA model is a variant of the LUE model originally proposed by Monteith (1972), in which NPP is the product of the photosynthetically active radiation (PAR) absorbed by green vegetation (APAR) and LUE:

$$\mathrm{NPP}(x,t) = \mathrm{PAR}(x,t) \times \mathrm{FPAR}(x,t) \times \varepsilon(x,t) \quad (1)$$

$$\varepsilon(x,t) = \varepsilon_{\max} \times T_{\varepsilon1}(x,t) \times T_{\varepsilon2}(x,t) \times W_{\varepsilon}(x,t), \quad (2)$$

where ε is the LUE and *FPAR* represents the fraction of absorbed *PAR* . It has been demonstrated in previous studies that APAR ($\mathrm{PAR} \times \mathrm{FPAR}$) is relatively easy to estimate from remotely sensed data because FPAR is a strong function of the normalized difference vegetation index (NDVI) (Goward and Huemmrich, 1992; Los, 1998; Sims et al., 2006b; Yu et al., 2009b). By comparison, ε has proved more difficult to estimate because it varies over seasons, biomes, or even species (Ahl et al., 2004; Sims et al., 2006b). Typical methods for estimating ε in the CASA model require prior specification of a maximum LUE ($\varepsilon_{\max}$) for a given biome. This maximum LUE has been downscaled by the temperature stress coefficient (TSC) and the moisture stress coefficient (MSC) (Eq. (2)) (Field et al., 1995; Potter et al., 1993). Early studies set $\varepsilon_{\max}$ to 0.405 g C/MJ (Potter et al., 1993) worldwide, but more recent studies have set $\varepsilon_{\max}$ to various values ranging from 0.389 to 0.978 g C/MJ for 13 types of biomes in East Asia (Yu et al., 2009b). Therefore, when $\varepsilon_{\max}$ is specified as a constant value for different biomes, the estimates of TSC and MSC are of key importance for using the CASA model. Generally, the two TSCs are relatively easily computed using the monthly mean temperature and the optimal temperature for plant growth, which is the temperature during the month of maximum NDVI (Piao et al., 2005; Potter et al., 1993). In comparison, an estimate of MSC can usually be obtained from a one-layer budget soil moisture model (SMM) (Malmström et al., 1997; Potter et al., 1993). However, an SMM always has a very complex model structure and needs many input soil parameters, including wilting coefficient, percentages of soil, sand, and clay particles, and soil depth (Saxton et al., 1986; Yu et al., 2009b) as well as monthly temperature and precipitation. Such data are often unavailable at sufficiently detailed spatial scales and are usually extracted from a soil class map with lower resolution in both space and time (Piao et al., 2005). Consequently, such data can introduce considerable errors into the output values of both MSC and final NPP and have been highlighted as one of the major limitations in the CASA model (Piao et al., 2005; Yu et al., 2009a,b), particularly when the model is implemented in specific ecoregions with a limited number of ground observations. Furthermore, no remote-sensing information was used in the MSC estimates in CASA, unlike the estimates of both APAR and TSC, which all include satellite NDVI data. Although it may be possible to improve the accuracy of MSC and final NPP outputs by improving the accuracy of soil parameters and climatic variables, it might be simpler and more direct to base the MSC estimates, at least partly, on remote-sensing data and thus undertake to provide continuous output with the same temporal and spatial resolution as the NDVI-used APAR and TSC.The land-surface water index (LSWI), a combination of the near-infrared and shortwave infrared bands, is a representative parameter of leaf and canopy water content as well as of soil moisture (Fensholt and Sandholt, 2003; Mao et al., 2014; Xiao et al., 2004a). The LSWI is based on the contrast between reflection in the infrared band caused by vegetation leaf cellular structure and absorption in the shortwave infrared band due to vegetation water content and soil moisture and can be calculated as $\mathrm{LSWI} = (\mathrm{NIR} - \mathrm{SWIR})/(\mathrm{NIR} + \mathrm{SWIR})$, where NIR and SWIR represent the reflectance in the near-infrared and shortwave infrared bands, respectively. A high index value indicates larger quantities of water in the canopy, whereas a low value indicates canopy water stress. In the vegetation photosynthesis model (VPM), developed to estimate gross primary productivity (GPP) proposed by Xiao et al. (2004a), the LSWI was successfully used to estimate the coefficient of water stress restriction on $\varepsilon_{\max}$ using the near-infrared (841–876 nm) and shortwave infrared bands (1628–1652 nm) of the Moderate Resolution Imaging Spectroradiometer (MODIS). This approach has been validated in various ecosystems, including evergreen needleleaf forest (Xiao et al., 2004a, 2005a), temperate deciduous forest (Wu et al., 2010b; Xiao et al., 2004b), tropical evergreen forest (Xiao et al., 2005b), and (semi-) arid grassland ecosystems (John et al., 2013). However, to date there is a dearth of information in the literature describing the use of LSWI to estimate MSC in the CASA model as well as in other remote-sensing-based NPP models. Furthermore, the VPM model that estimates GPP based on LSWI has been used only at the very small scale of a flux tower footprint, which is generally <1 km and cannot provide truly per-pixel GPP output (Rahman et al., 2005). Therefore, large-scale LSWI applications (per pixel) need to be further tested for both NPP and GPP modeling, particularly with the aim of providing a MSC with the same spatial and temporal resolution as NDVI data, which is used to estimate APAR and TSC.

Due to the limitation of estimating MSC in the CASA model (Yu et al., 2009b), an effort has been made in this research to improve and evaluate the CASA model by introducing LSWI (an LSWI-based CASA model) derived from the MODIS near-infrared and shortwave infrared bands, with a 500 m spatial resolution and a monthly interval, to quantify the spatial changes in the NPP of terrestrial ecosystems in the (semi-) arid climate of the Mongolian Plateau. To the best of our knowledge, this is the first study to downscale the ε_{max} in the CASA model by introducing LSWI and to simulate vegetation NPP at a truly per-pixel scale based on LSWI (i.e., at large spatial extent) in arid and semiarid ecosystems. The result will not only explore an alternative method for estimating the MSC in the CASA model, but also provide a finer spatial (500 m × 500 m) and temporal (monthly) resolution NPP output than the MOD17A3 product (1 km × 1 km and yearly) in the plateau.

1.1. Data and methods

1.1.1. Study area

The Mongolian plateau is located in a transitional belt extending from the Gobi Desert of Central Asia to the Siberian taiga forest from south to north and covers an area of approximately 2.7 million km^2. It is occupied by the Inner Mongolia Autonomous Region, China in the southeast (1.2 million km^2), and Mongolia in the northwest (1.5 million km^2) (Bao et al., 2014) (Fig. 1). The plateau is governed by a typical continental climate regime with extremely cold winters and warm summers (Angerer et al., 2008). The multi-year mean precipitation varies from <50 mm in the southwestern Gobi Desert to >400 mm in the northeastern forests. Annual mean temperature is primarily latitude-dependent, ranging from approximately 1.5 °C in the northern mountains to 16 °C in the southwestern Gobi Desert. Due to the arid and semiarid climate, steppe grassland is the dominant ecosystem type, covering about 84% and 66% of the total territories of, respectively, Mongolia and Inner Mongolia, except for the northern (Mongolia) and northeastern (Inner Mongolia) forested area and the southwestern Gobi Desert (Angerer et al., 2008; Bao et al., 2015; Wang et al., 2013). Because the plateau is shared by two different entities (Mongolia and Inner Mongolia, China) with different economic and social organizations, the plateau ecosystems are subject to different human populations and anthropogenic impacts on the two sides of the international border (Neupert, 1999). In the northern part of the plateau, Mongolia still harbors vast, high-quality grasslands with nomadic pastoralism from ancient times until now that represent rare reference ecosystems in near-natural condition for ecological modeling and climate change studies (Zemmrich et al., 2010). Furthermore, the population of Mongolia was 2.83 million in 2011, with the lowest density in the world, 1.8 persons per square kilometer (Mongolian Statistical Yearbook, 2011). In the southern Inner Mongolia region, on the contrary, the nomadic pastoralism of the past has changed to sedentary village-based pasturing with relatively higher population density and pressure on natural resources. This difference makes the plateau an ideal region for comparing both ecological models and ecosystem evolution trends under different human pressures (Bao et al., 2014).

1.2. Dataset and pre-processing

1.2.1. MODIS reflectance data

The 8-day Terra MODIS surface reflectance atmospheric correction algorithm product (MOD09A1) with a resolution of 500 m × 500 m and with seven bands from optical to shortwave ranges for 2009 (because the field data were collected in late July and early August 2009) was used to derive the NDVI and LSWI, which were then used to parametrize the CASA model based on the following equations:

$$\mathrm{NDVI} = \frac{(R_2 - R_1)}{(R_2 + R_1)} \tag{3}$$

$$\mathrm{LSWI} = \frac{(R_2 - R_6)}{(R_2 + R_6)}, \tag{4}$$

where R_x represents the reflectance in a given band of the MODIS data. To decrease non-vegetation effects in the MODIS-derived NDVI and to model the NPP at monthly scale, growing-season monthly NDVI and LSWI data were generated by applying the maximum value composite (MVC) method (Holben, 1986) to several images for each growing-season month. The growing season was phenologically defined as the period from April to October, and this season was the focus of this study because during winter most plants in the plateau are covered by snow and almost all photosynthesis ceases (Bao et al., 2014).

1.2.2. Meteorological data

The meteorological data supplied to drive the CASA model included growing-season monthly mean temperatures, monthly precipitation amounts, and monthly solar radiation. These data were derived from 108 meteorological stations (Inner Mongolia: 48, Mongolia: 60) and 22 solar radiation observation stations (Inner Mongolia: 8, Mongolia: 14) across the plateau (Fig. 1) and were provided by the Mongolian and Inner Mongolian Weather Bureaus. These data were interpolated in the ArcGIS environment using the kriging method at a spatial resolution of 500 m to match the NDVI and LSWI both temporally and spatially and to implement the CASA model at the pixel scale. Solar radiation was converted to PAR by multiplying by 0.5 (Piao et al., 2005). Although some errors may have resulted from a real interpolation due to the limited number of meteorological stations available (Piao et al., 2005), the kriging method has been recommended as a better interpolation method with higher accuracy and lower bias than other methods (Li et al., 2005), particularly in regions where elevation changes are minimal (mostly grassland ecosystems) like the Mongolian Plateau (Bao et al., 2015).

1.2.3. Vegetation type

Vegetation type data were obtained from the National Atlas of Mongolia (Institute of Geography, Mongolian Academy of Science, 2009), and a vegetation map of Inner Mongolia with a scale of 1:1000000 was used to set the maximum LUE and to analyze NPP variations at the biome scale. The vegetation map was first scanned, geometrically corrected, mosaicked, and digitized using the ArcGIS software and then rasterized at 500 m, as was done for the climatic datasets. As in previous studies (Bao et al., 2014, 2015), vegetation types in the plateau were further grouped into coniferous forest, broadleaf forest, shrubs, meadow, steppe, desert steppe, alpine steppe, sandy land vegetation, and crops (Fig. 1). Gobi Desert vegetation was neglected in the present study because it was extremely sparse.

1.2.4. Field observation data

To validate the results of the LSWI-based CASA model, two types of field-observed biomass values were collected. The first type, provided by the Inner Mongolia Institute of Grassland Survey and Planning, was the aboveground biomass (AGB) measured in 147 plots (1 m × 1 m) in the Hulunbuir and Xilingol grasslands and the Ordos Plateau in August 2009, covering meadow, typical steppe, and desert steppe (Fig. 1). The second type was the aboveground and belowground biomass (BGB) measured in 12 plots (1 m × 1 m) in August 2012 in the Hulunbuir grasslands of Inner Mongolia. Considering that some sampling sites were very close to roads and villages or were located within cultivated farms or forests (and therefore subject to human disturbance) (Xie et al., 2009), 101 of the 147 samples used as validation plots and 46 plots were discarded in 2009. The biomass was hand-harvested at the ground surface and was oven-dried at 65 °C until a constant dry biomass value

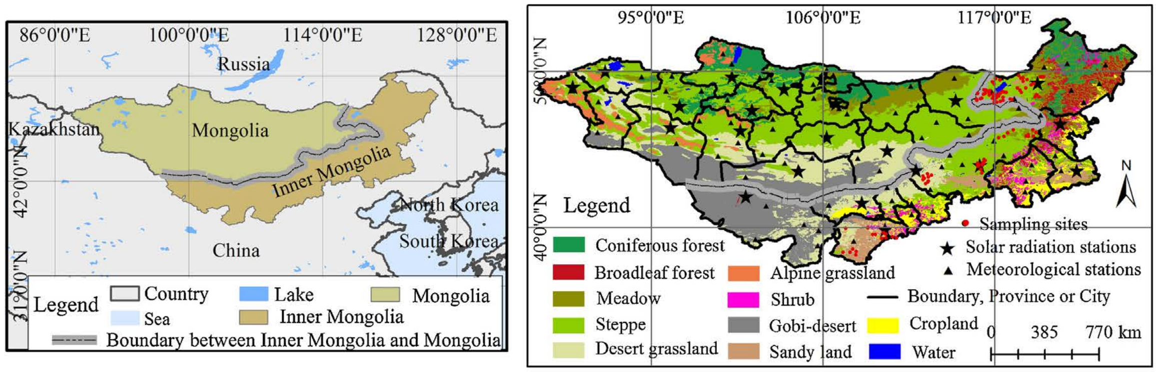

Fig. 1. Location of the study area and the spatial pattern of vegetation types, with the distribution of meteorological stations and sampling sites.

was recorded. Because the model-simulated NPP includes both the aboveground NPP (ANPP) and the belowground NPP (BNPP), the field-observed biomass values in 2009 were converted to NPP according to the method proposed by Gill et al. (2002); Eqs. (5)–(7) and the ratio of BGB to AGB determined for different steppe grassland types. The ratio was set to 3.982 for typical steppe as calculated from data for 12 plots in 2012 and to 5.26 and 7.89, respectively, for meadow and desert steppe, a set of values proposed by Piao et al. (2007), because all sampling plots are located within these three types of grasslands:

$$\mathrm{NPP} = \mathrm{ANPP} + \mathrm{BNPP} \tag{5}$$

$$\mathrm{BNPP} = \mathrm{BGB} \times \left(\frac{\mathrm{liveBGB}}{\mathrm{BGB}}\right) \times \mathrm{turnover} \tag{6}$$

$$\mathrm{turnover}{=}0.0009(\mathrm{gm}^{-2}) \times \mathrm{ANPP} + 0.25, \tag{7}$$

where liveBGB is the living BGB for a current year, liveBGB/BGB was set to 0.6 according to the results reported by Gill et al. (2002), and turnover is grassland root turnover. AGB was converted to ANPP using a conversion factor of 0.475 (Scurlock et al., 1999).

1.3. Method

1.3.1. Justification of the approach used to estimate a modified MSC in the CASA model

In early CASA models, the MSC was calculated as:

$$W_{\varepsilon}(x,t) = 0.5 + 0.5 \times \frac{\mathrm{EET}(x,t)}{\mathrm{PET}(x,t)}, \tag{8}$$

where EET and PET represent the estimated and potential evapotranspiration and are usually determined from the one-layer budget SMM (Piao et al., 2005; Potter et al., 1993). The value of $W_{\varepsilon}(x,t)$ usually varies from 0.5 in very arid ecosystems to 1 in very wet ecosystems. According to this logic, the potential use of per-pixel W_{vpm} in the VPM model (Eq. (9)) proposed by Xiao et al. (2004a) was investigated for estimating a per-pixel MSC in the CASA model. It was found that per-pixel W_{vpm} values are simply contraries of $W_{\varepsilon}(x,t)$ (Eq. (8)) and range from 0 in very wet ecosystems to 1 in very arid ecosystems. This may be a major limitation of the VPM model when implemented at a per-pixel scale:

$$W_{\mathrm{vpm}} = \frac{1 + \mathrm{LSWI}}{1 + \mathrm{LSWI}_{\mathrm{max}}}, \tag{9}$$

where $\mathrm{LSWI}_{\mathrm{max}}$ represents the maximum LSWI within the growing season for individual pixels and is estimated using the MVC method (Holben, 1986). According to the principle of $W_{\varepsilon}(x,t)$ in the early CASA models, which varied from 0.5 in very arid ecosystems to 1 in very wet ecosystems, the values of W_{vpm} were accordingly inverted to match the range of $W_{\varepsilon}(x,t)$ values as follows:

$$W_{\mathrm{vpm\_inversed}} = \left(1 - \frac{1 + \mathrm{LSWI}}{1 + \mathrm{LSWI}_{\mathrm{max}}}\right) + 0.5, \tag{10}$$

Although LSWI and the derived $W_{\mathrm{vpm\_inversed}}$ can capture the gradient and the variations in hydrothermal ecosystem conditions, it has also been suggested that precipitation has a profound impact on vegetation productivity, and therefore that incorporation of precipitation information into ecosystem models can help to improve the accuracy of vegetation productivity determinations (Wu and Chen, 2012), particularly in arid and semiarid ecosystems (Thomey et al., 2011; Wu and Chen, 2012). Therefore, here the use of $W_{\mathrm{vpm\_inversed}}$ was further justified by incorporating precipitation regimes. As a meteorological scalar that mostly ranges from 0 to 1, a simple precipitation scalar (ScaledP) was first proposed as:

$$\mathrm{ScaledP} = \frac{\mathrm{prec}}{\mathrm{prec}_{\mathrm{max}}}, \tag{11}$$

where prec represents the monthly precipitation amounts and $\mathrm{prec}_{\mathrm{max}}$ is the maximum monthly precipitation within the growing season for individual pixels of interpolated precipitation. Based on the two scalars, $W_{\mathrm{vpm\_inversed}}$ and ScaledP, a modified MSC (W_{lswi}) algorithm was then proposed by multiplying $W_{\mathrm{vpm\_inversed}}$ by ScaledP as follows:

$$W_{\mathrm{lswi}} = W_{\mathrm{vpm\_inversed}} \times \mathrm{ScaledP} + 0.5, \tag{12}$$

where the constant 0.5 ensures that W_{lswi} ranges between 0.5 in very arid ecosystems and 1 in very wet ecosystems, similarly to the early CASA model (Potter et al., 1993; Yu et al., 2009b). Once the modified W_{lswi} was determined, the improved CASA model, called the LSWI-based CASA model, was applied directly to the ecosystems of the Mongolian Plateau without changing the estimates of other variables in the algorithm, including APAR and the two TSCs. In the present study, $\varepsilon_{\mathrm{max}}$ was set equal to the values (Table 1) proposed by Zhu et al. (2006) for the whole of China according to the vegetation types of the plateau.

1.3.2. Evaluation of model performance

Two methods were used to evaluate the performance of the LSWI-based CASA model. In the first method, the modeled NPP values were compared with those actually measured in 2009 (Fig. 1) from 101 ground plots and the correlation coefficient and significance level and root mean square error (RMSE) between the two groups of data were examined (Huang et al., 2010; Mu et al., 2013a; Xie et al., 2009). Because determining which pixel a particular ground plot fell into was difficult, average values of nine pixels (3 × 3) of modeled NPP values were extracted according to the location of the ground plot to represent the modeled NPP (Rahman et al., 2005). In the second evaluation, the results from

Table 1
Maximum light-use efficiency of different biomes (CF: coniferous forest, BD: broadleaf forest, SB: shrubs, MD: meadow, ST: steppe, DS: desert steppe, AS: alpine steppe, SLV: sandy land vegetation, CP: crops).

	CF	BF	SB	MD	ST	DS	AS	SLV	CP
ε_{max}	0.485	0.692	0.429	0.542	0.542	0.542	0.542	0.542	0.542

the LSWI-based CASA model were compared with those from the CASA model as proposed by Yu et al. (2009b) (the Yu-CASA model). This was one of the acceptable ways to proceed when large-scale synchronous ground data for whole biome types were unavailable (Wu et al., 2010b; Xie et al., 2009). To ensure comparability of results from the two models, here we used absolutely identical data sets to parameterize the two versions of CASA models, except for MCS. The comparison between the two models was performed at the biome scale and at the per-pixel scale, respectively, in the plateau.

2. Results

2.1. Field sample-based accuracy validation of the two CASA models

Validation was conducted by comparing the ground observed NPP values from 101 plots covering meadow, typical steppe, and desert steppe in Inner Mongolia in August 2009 with the modeled NPP from both the LSWI-based CASA model and the Yu-CASA model (Fig. 2). Even though no significant improvement in R-value ($R^2 = 0.717$, $p < 0.001$) was observed in the LSWI-based CASA model (Fig. 2a), the proposed method achieved results comparable to those from the Yu-CASA model ($R^2 = 0.714$, $p < 0.001$) (Fig. 2b). Generally, both models tended to; underestimate NPP when the observed NPP was >120 g C/m^2/Aug, overestimate when the observed NPP was <45 g C/m^2/Aug in Inner Mongolian grasslands, and to generate predictions close to observed values when the observed NPP were located in the vicinity of 70 g C/m^2/Aug. The *RMSEs* between the observed and modeled NPP from the two models were 26.2 and 27.9 g C/m^2, respectively.

2.2. Comparison of predictions between the LSWI-based CASA model and the Yu-CASA model by biome type

Comparison of the monthly time trends of NPP for each biome at a monthly scale (Fig. 3) shows a good general correspondence between NPP as modeled by the LSWI-based CASA model and the Yu-CASA model, particularly in spring (April–May) and in autumn (September–October), indicating that the two models were similar in terms of their ability to predict monthly changes in NPP for each biome type. However, the LSWI-based CASA model tended to overestimate NPP slightly in the summer months; this bias was most evident in July for desert steppe (Fig. 3e) and alpine steppe (Fig. 3i). A simple linear regression model by biome type further showed good agreement between the two models during the growing season in 2009, with R^2 values ranging from 0.980 in alpine steppe to 0.998 in typical steppe (Table 2). The *RMSE* s between the two models for modeled NPP ranged from 3.24 to 15.52 g C/m^2/month in desert steppe and alpine steppe, respectively (Table 2).

Table 2
Correlation coefficients and RMSE (g C/m^2/month) between the LSWI-based CASA modeled NPP and the Yu-CASA modeled NPP.

Vegetation type	Correlation coefficient (R^2)	RMSE (g C/m^2/month)
Coniferous forest	0.996***	6.58
Broadleaf forest	0.983***	10.56
Meadow steppe	0.994***	5.90
Typical steppe	0.998***	6.39
Desert steppe	0.985***	3.24
Alpine steppe	0.980***	15.52
Shrubs	0.997***	3.59
Sandy land vegetation	0.994***	5.67
Crops	0.995***	6.65
All vegetation	0.982***	13.44

*** Indicates $p<0.01$.

2.3. Per-pixel comparison between NPP modeled by the LSWI-based CASA model and the Yu-CASA model

Comparison of spatially explicit maps from different models can provide further insight into fine distinctions in the spatial output patterns from different models (Xie et al., 2009). The spatial pattern of the total NPP in the 2009 growing season modeled by the LSWI-based CASA model (Fig. 4a) and the Yu-CASA model (Fig. 4b) were compared at the per-pixel scale. To ensure spatial pattern comparability of the results from the two models, the same density slice (legend of the two maps) was used to map the final NPP. When comparing the NPP maps generated by the two models, it is clear that very similar spatial patterns can be observed in the two NPP maps in terms of both the spatial distribution and NPP values (Fig. 4a, b), indicating that the predictions of these models are consistent and comparable with each other in the Mongolian Plateau. The average NPP modeled by the Yu-CASA and LSWI-based CASA models was approximately 216.2 and 232.6 (g C/m^2/April–August), respectively. There was only a difference of around 16 g C in the growing-season sum NPP, or approximately 2.3 g C bias per month. Consistently with the vegetation gradient (Fig. 1), the NPP exhibited a decreasing trend from northeast to southwest (Inner Mongolia) and from north to south (Mongolia). The highest NPP values, >400 g C/m^2/April–August, tended to concentrate in northern Mongolia and northeastern Inner Mongolia, in areas with high-density forest. The moderately high values, ranging from 100 to 400 g C/m^2/April–August, were mostly distributed over the central parts of the plateau, where the land is dominated by meadow steppe, typical steppe, crops, and shrubs. The lowest values, <100 g C/m^2/April–August, were generally observed in the dry grasslands and desert regions (Gobi Desert) of the southern and western regions of the plateau. Furthermore, very high per-pixel correlations can also be observed between the NPP modeled by the two models (Fig. 4c), with R values >0.98 over most of the study region, except for relatively lower values in the southwestern Gobi Desert. However, R values in this region are >0.85 and are significant at the 0.001 level.

3. Discussion

3.1. Field sample-based accuracy evaluation

A modified version of the CASA model was proposed and tested by adjusting the MSC of the early CASA model (Potter et al., 1993), and the results were compared with the results of the Yu-CASA model (Yu et al., 2009b). The accuracy of the two models was validated using the same ground-observed NPP data derived from 101 sampling sites covering three types of grassland in Inner Mongolia. The R^2 and *RMSE* values between both the LSWI-based CASA and the Yu-CASA model and the observed NPP were approximately equal, indicating that the predictions of these models were relatively stable and similar (Fig. 2). The results of the two models were also

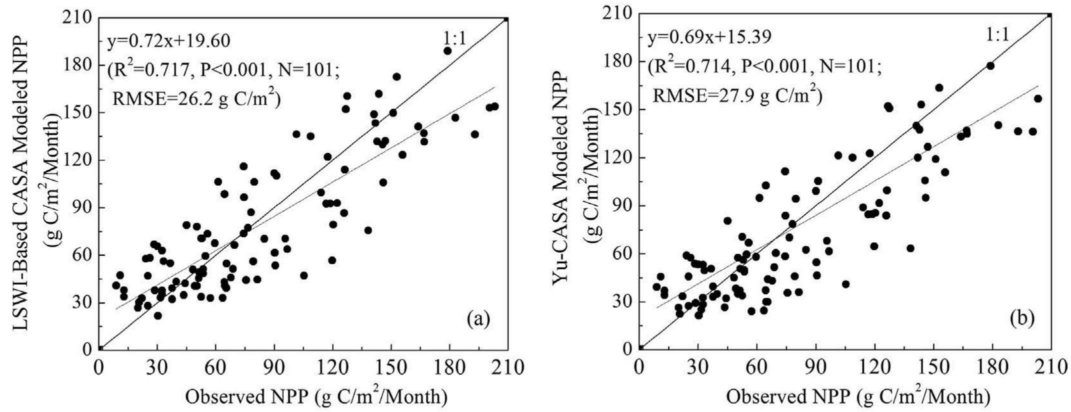

Fig. 2. Accuracy validation of modeled NPP estimated from the LSWI-based CASA model (a) and the Yu-CASA model (b).

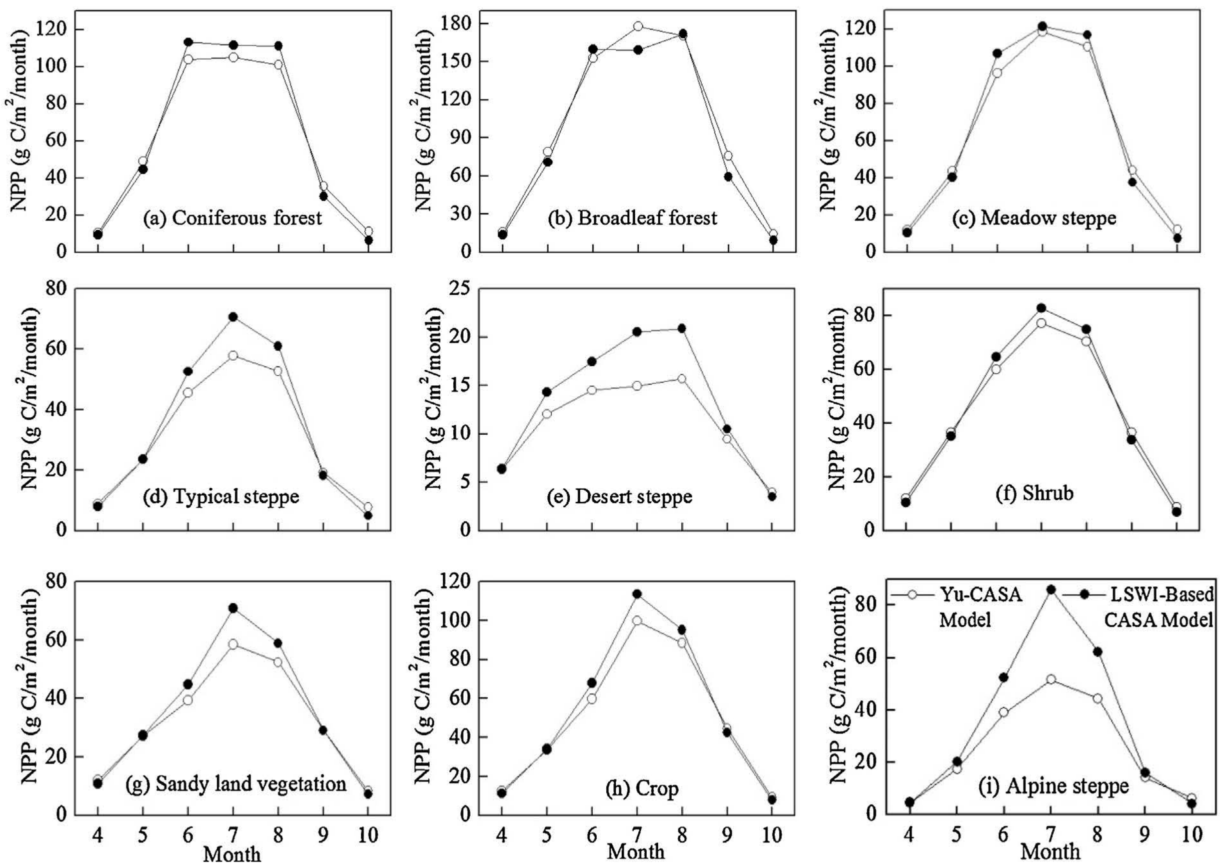

Fig. 3. Comparison of monthly variation between the LSWI-based CASA modeled and Yu-CASA modeled NPP by biome type. (a) Coniferous forest, (b) Broadleaf forest, (c) Meadow steppe, (d) Typical steppe, (e) Desert steppe, (f) Shrub, (g) Sandy land vegetation, (h) Crop and (i) Alpine steppe.

comparable to results from previous studies in Inner Mongolia (Mu et al., 2013a,b) and in the Qinghai-Tibet Plateau (Fan et al., 2010). The results showed satisfactory agreement (correlation coefficients between modeled and observed NPP) with studies of year-to-year NPP variation if considering the errors of both the modeling process and field observations (Fan et al., 2010; Mu et al., 2013a). However, compared to the earlier CASA model, the accuracy of the proposed LSWI-based CASA model, which adjusted the structure and parameters for estimating the MSC, was not improved significantly (Fig. 2a) as measured by the correlation coefficient with observed NPP. However, MSC estimation was greatly simplified (Eq. (12)), not only in model structure, but also in model execution compared to the original logic of the CASA model, which normally used a complex SMM (Field et al., 1995; Piao et al., 2005; Potter et al., 1993) or a large amount of external climate data (Yu et al., 2009b) to estimate the MSC. However, some concern may arise from the fact that the accuracy evaluation was not performed at a plateau scale or in other specific biomes, including forest, cropland, and shrubland. These limitations are not advisable, but were necessitated by the limited number of acceptable samples due to the restricted accessibility of certain areas and the lack of corresponding observational data (Xie et al., 2009). These limitations are especially prevalent in regions like the Mongolian Plateau which links two countries (Bao et al., 2014) and where most of the plateau is covered by steppe grasslands (about 84% and 66% of the total territories of Mongolia and Inner Mongolia), except for a small number of forested areas

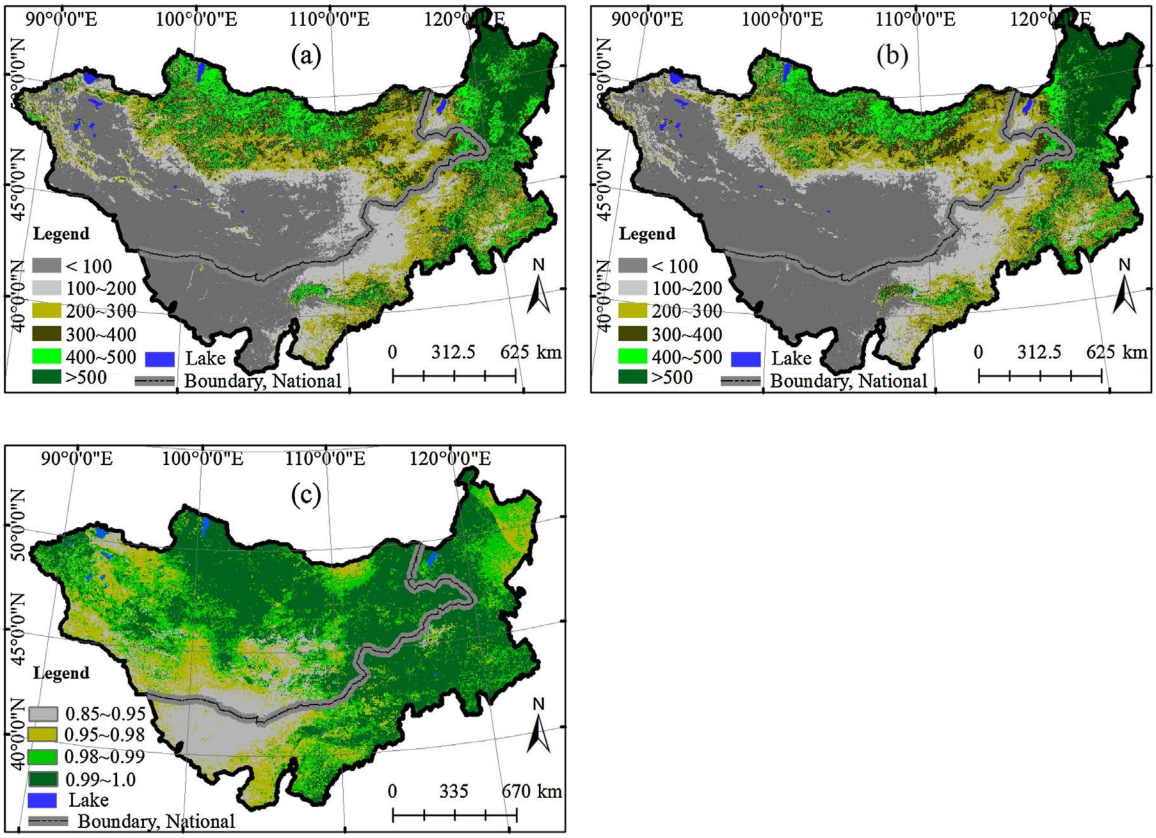

Fig. 4. Spatial patterns of growing-season total NPP in the Mongolian Plateau as modeled by the LSWI-based CASA model (a) and the Yu-CASA model (b), and per-pixel correlation coefficients between NPP as modeled by the two models (c).

and the Gobi Desert (Angerer et al., 2008; Bao et al., 2015; Wang et al., 2013). In such cases, a comparison with other relevant models is one of the most widely used methods (Xie et al., 2009; Zhu et al., 2006) and can be used to test model accuracy and stability in previous studies (Xie et al., 2009).

3.2. Comparison between the LSWI-based CASA model and the Yu-CASA model

Regardless of the kind of comparison (per-pixel or by biome type) between the LSWI-based CASA model and the Yu-CASA model, a very high level of correspondence was found between the outputs. This indicates that the LSWI-based CASA model proposed here has strong potential as an alternative method to estimate the NPP of a wide range of vegetation types at the scale of the entire Mongolian Plateau. Furthermore, it also indicates the comparability of the two models to capture the phenological NPP growth cycle (Fig. 3). The spatial NPP distribution patterns and values from the two models for the Mongolian Plateau are not only in accordance with each other, but are also consistent with the results obtained by Yu et al. (2009b) and Matsushita and Tamura (2002), which were obtained for the entire East Asian ecosystem. The growing-season mean NPP values (216.2 g C/m^2/April–August [the Yu-CASA model] and 232.6 g C/m^2/April–August [the LSWI-based CASA model]), are generally located in the range (200.34–251.72 g C/m^2/year from 2003 to 2008) observed in Inner Mongolia. Furthermore, the growing-season mean NPP values are spatially consistent with the distribution in Inner Mongolia, particularly in the forest area of northeast Inner Mongolia, as reported by Li et al. (2013), with a value of >500 g C/m^2/April–August. The NPP values are also similar to the results from Mu et al. (2013a) in Inner Mongolia that ranged from 235.0 to 271.6 g C/m^2/year during the period 1985–2009. However, compared to the proposed method for estimating the MSC, models like the early version of the CASA model (Field et al., 1995; Potter et al., 1993) or the improved CASA model for the ecosystems of East Asia (Yu et al., 2009b) and Inner Mongolia (Li et al., 2013) require multiple input parameters to estimate the MSC, and these parameters are often difficult to obtain, particularly when the study area covers more than one country, as is the case in the Mongolian Plateau. The LSWI-based CASA model was optimized for NPP modeling in arid and semiarid regions by introducing LSWI ($W_{\text{vpm\_inverse}}$) and ScaledP to account for the effects of moisture condition, which is a key parameter in dryland regions (Wu and Chen, 2012) and adjusting maximum LUE in the early CASA model. This may be an improvement in NPP modeling over the CASA model, although LSWI is widely used in GPP modeling (Xiao et al., 2004a) color of this citition. In particular, the use of LSWI at the per-pixel scale, which has been used in previous studies only for a flux tower footprint with a relatively limited spatial coverage (John et al., 2013; Wu et al., 2010a,b; Xiao et al., 2005b), can provide a MSC with continuous spatial coverage, and a high degree of spatial variability can be observed at the per-pixel scale (Fig. 5a). However, a MSC that is totally derived from climatic variables or SMMs (Piao et al., 2005; Yu et al., 2009b) always has spatial discontinuities (Fig. 5b) (e.g., differences between each density slice) due to the interpolation of all climatic variables and soil parameters. This discontinuity may raise some uncertainties about output ecosystem productivity (Gu et al., 2013). Precipitation variability has been shown to have a significant effect on ecosystem productivity (Beer et al., 2010). The scaling method for precipitation quantities (Eq. (11)) proposed here to estimate the MSC is similar to the scaling method for precipitation intensity proposed by Wu and Chen (2012), who reported that scaling precipitation could correct for regional differences and improve the precision of monthly GPP estimates by 10% in four

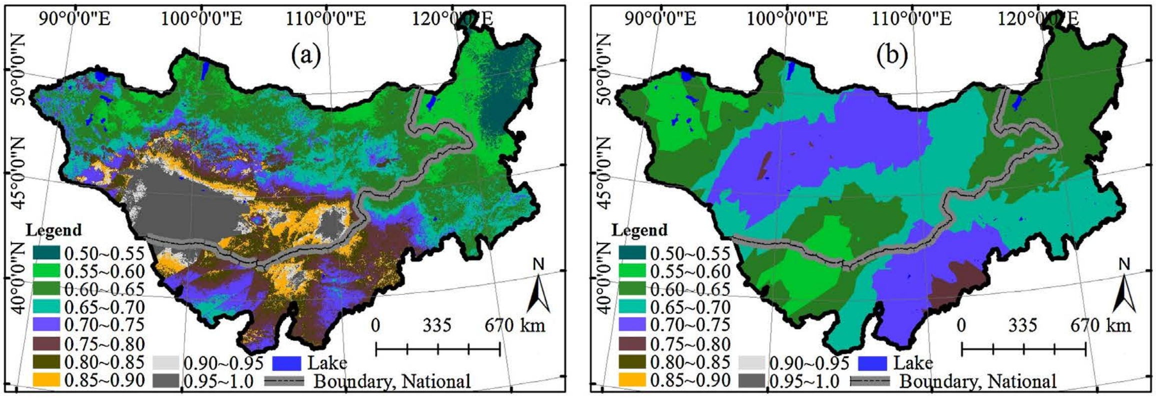

Fig. 5. Spatial pattern of MSCs in the Mongolian Plateau as calculated by the proposed LSWI-based CASA model (a) and the Yu-CASA model (Yu et al., 2009b) (b). (May 2009 was taken as an example).

North American grasslands. Use of LSWI and scaled precipitation in this study has further confirmed the results of these earlier GPP modeling studies (John et al., 2013; Wu and Chen, 2012; Xiao et al., 2004a) and has also extended their utility to NPP modeling, particularly at the per-pixel scale, which has been highlighted as one of the major limitations in the use of LSWI in earlier studies (Rahman et al., 2005).

3.3. Potential future challenges for the proposed MSC

Although it has been suggested that the results presented in this study might provide a first case study of the utility of LSWI and scaled precipitation in NPP modeling of the arid and semiarid climate of the Mongolian Plateau, specific attention has also been paid to future analysis. Firstly, the feasibility of any improvements to the modified model needs to be further tested in other ecosystems, even globally, as has been done for the VPM model (John et al., 2013; Xiao et al., 2004a,b, 2005b), because vegetation under specific hydrothermal conditions always has different response characteristics to climatic variables and hydrothermal conditions (Bao et al., 2015; Chuai et al., 2012; Mao et al., 2014). This is a possible reason for the different responses of LUE to varying hydrothermal conditions over both space and time (Sims et al., 2006a; Wu and Chen, 2012). Use of LSWI and scaled precipitation in the Mongolian Plateau can only serve as a representative sample of ecoregions with an arid and semiarid climate. Secondly, although the scaled LSWI (W_{vpm}) (Eq. (9)) was directly used to adjust the maximum LUE in the VPM model (Xiao et al., 2004a,b, 2005b), it seems inappropriate to adjust the maximum LUE in the CASA model directly (Potter et al., 1993) because the spatial distribution of W_{vpm} at the per-pixel scale ranges from 0 in very wet ecosystems to 1 in very arid ecosystems. This may be one of the most important considerations in using LSWI at the per-pixel scale, not only in VPM models, but also in other related ecosystem models. Thirdly, LSWI was chosen to adjust the maximum LUE according to the results from previous studies that suggested that the LSWI is more sensitive to leaf and canopy water content and soil moisture variation than the normalized difference water index (NDWI, NDWI = $\left(\rho 0.86 - \rho 1.24/\rho 0.86 + \rho 1.24\right)$) (Xiao et al., 2005a), particularly in semiarid environments (Fensholt and Sandholt, 2003). However, the preliminary comparisons among NDWI, LSWI, moisture stress index, global vegetation moisture index and canopy water content and soil moisture variation in different ecosystems needs to be further explored, particularly at the per-pixel level for large-scale application. More field work is needed to collect multi-scale data on soil moisture and foliage water content and to explore their relationship with the water index described above. The last consideration is the underlying mechanism between LUE and LSWI and scaled precipitation. Although reasonable results were observed here compared with the Yu-CASA model and field observation data, it is still unclear why larger differences were observed in summer months (July–August) in alpine steppes (Fig. 3i). Although these may have been caused by the higher LSWI value due to the permanent snow cover in some higher mountain areas where alpine steppe is distributed (Li et al., 2007), this observation still indicates that further analysis and validation are needed to clarify how LSWI and scaled precipitation impact the LUE. Unknown mechanisms are always an impediment to further modification of a model (Wu and Chen, 2012).

4. Conclusions

This study proposed a new method (the LSWI-based CASA model) to estimate regional NPP for the Mongolian Plateau ecosystems with an arid and semiarid climate using MODIS reflectance data and climatic variables (PAR, temperature, and precipitation) and compared the results with those from the Yu-CASA model and field observation data. The proposed method improved the MSC calculation by using satellite remote sensing-derived LSWI and precipitation instead of values from SMMs or climate-dependent models and can offer a cost-effective solution for estimating the MSC. Both models are based on the principle of the LUE model originally proposed by Monteith (1972) and can provide comparable results for NPP in the Mongolian Plateau. The results obtained indicate reasonable agreement between field-observed NPP and NPP as predicted by the LSWI-based CASA model and the Yu-CASA model, indicating the potential for these LUE models to simulate NPP in semiarid ecoregions. These results will be useful for the development of future NPP models based entirely on remote-sensing observations. However, some differences and uncertainties in NPP output were found to exist between the LSWI-based CASA model and the Yu-CASA model, particularly in specific biomes in summer. It remains unclear which model is the most accurate predictor of NPP in some specific biomes due to a lack of timely and synchronous NPP values from field observations with remote-sensing imagery. Therefore, further modeling efforts should be concentrated primarily on years and months in the same ecoregions and on other ecosystems, as done in previous studies using the VPM model.

Acknowledgements

This study was supported by the National Natural Science Foundation of China (grant No. 41301456), the National "Twelve-five" Technology Support Project of China (grant No. 2013BAK05B01), and the Key Technologies R&D Program of China (grant No. 2012BAC19B04 & 2013BAC03B00). We would like to thank the anonymous reviewers for providing constructive suggestions, and also to thank the MODIS science teams for providing accessible data products.

References

Ahl, D.E., Gower, S.T., Mackay, D.S., et al., 2004. Heterogeneity of light use efficiency in a northern Wisconsin forest: implications for modeling net primary production with remote sensing. Remote Sens. Environ. 93, 168–178.
Angerer, J., Han, G., Fujisaki, I., et al., 2008. Climate change and ecosystems of Asia with emphasis on Inner Mongolia and Mongolia. Rangelands 6, 46–51.
Bao, G., Bao, Y., Sanjjav, A., et al., 2015. NDVI-indicated long-term vegetation dynamics in Mongolia and their response to climate change at biome scale. Int. J. Climatol. 35, 4293–4306.
Bao, G., Qin, Z., Bao, Y., et al., 2014. NDVI-based long-term vegetation dynamics and its response to climatic change in the Mongolian Plateau. Remote Sens. 6, 8337–8358.
Beer, C., Reichstein, M., Tomelleri, E., et al., 2010. Terrestrial gross carbon dioxide uptake: global distribution and covariation with climate. Science 329, 834–838.
Chuai, X.W., Huang, X.J., Wang, W.J., Bao, G., 2012. NDVI, temperature, and precipitation changes and their relationships with different vegetation types during 1998–2007 in Inner Mongolia, China. Int. J. Climatol. 33, 1696–1706.
Fan, J.-W., Shao, Q.-Q., Liu, J.-Y., et al., 2010. Assessment of effects of climate change and grazing activity on grassland yield in the three rivers headwaters region of Qinghai-Tibet Plateau, China. Environ. Monit. Assess. 170, 571–584.
Fensholt, R., Sandholt, I., 2003. Derivation of a shortwave infrared water stress index from MODIS near- and shortwave infrared data in a semiarid environment. Remote Sens. Environ. 87, 111–121.
Fensholt, R., Sandholt, I., Rasmussen, M.S., et al., 2006. Evaluation of satellite-based primary production modelling in the semi-arid Sahel. Remote Sens. Environ. 105, 173–188.
Field, C.B., Randerson, J.T., Malmström, C.M., 1995. Global net primary production: combining ecology and remote sensing. Remote Sens. Environ. 51, 74–88.
Gill, R., Kelly, R., Parton, W., et al., 2002. Using simple environmental variables to estimate below-ground productivity in grasslands. Global Ecol. Biogeogr. 11, 79–86.
Goward, S.N., Huemmrich, K.F., 1992. Vegetation canopy PAR absorbance and the normalized difference vegetation index: an assessment using the SAIL model. Remote Sens. Environ. 39, 119–140.
Gu, Y., Wylie, B.K., Bliss, N.B., 2013. Mapping grassland productivity with 250-m eMODIS NDVI and SSURGO database over the Greater Platte River Basin, USA. Ecol. Indic. 24, 31–36.
Hazarika, M.K., Yasuoka, Y., Ito, A., et al., 2005. Estimation of net primary productivity by integrating remote sensing data with an ecosystem model. Remote Sens. Environ. 94, 298–310.
Hicke, J.A., Asner, G.P., Randerson, J.T., et al., 2002. Trends in North American net primary productivity derived from satellite observations, 1982–1998. Global Biogeochem. Cycles, 16, 2–1 to 2–14.
Holben, B.N., 1986. Characteristics of maximum-value composite images from temporal AVHRR data. Int. J. Remote Sens. 7, 1417–1434.
Huang, N., Niu, Z., Wu, C., et al., 2010. Modeling net primary production of a fast-growing forest using a light use efficiency model. Ecol. Modell. 221, 2938–2948.
John, R., Chen, J., Noormets, A., et al., 2013. Modelling gross primary production in semi-arid Inner Mongolia using MODIS imagery and eddy covariance data. Int. J. Remote Sens. 34, 2829–2857.
Li, J., Cui, Y., Liu, J., et al., 2013. Estimation and analysis of net primary productivity by integrating MODIS remote sensing data with a light use efficiency model. Ecol. Modell. 252, 3–10.
Li, X., Cheng, G., Lu, L., 2005. Spatial analysis of air temperature in the Qinghai-Tibet Plateau. Arct. Antarct. Alp. Res. 37, 246–252.
Li, Z., Yu, G., Xiao, X., et al., 2007. Modeling gross primary production of alpine ecosystems in the Tibetan Plateau using MODIS images and climate data. Remote Sens. Environ. 107, 510–519.
Lobell, D.B., Hicke, J.A., Asner, G.P., et al., 2002. Satellite estimates of productivity and light use efficiency in United States agriculture, 1982–98. Global Change Biol. 8, 722–735.
Los, S.O., 1998. Linkages between global vegetation and climate: an analysis based on NOAA advanced very high resolution radiometer data. In: PhD Dissertation. National Aeronautics and Space Administration (NASA).
Malmström, C.M., Thompson, M.V., Juday, G.P., et al., 1997. Interannual variation in global-scale net primary production: testing model estimates. Global Biogeochem. Cycles 11, 367–392.
Mao, D., Wang, Z., Li, L., et al., 2014. Spatiotemporal dynamics of grassland aboveground net primary productivity and its association with climatic pattern and changes in Northern China. Ecol. Indic. 41, 40–48.
Matsushita, B., Tamura, M., 2002. Integrating remotely sensed data with an ecosystem model to estimate net primary productivity in East Asia. Remote Sens. Environ. 81, 58–66.
Monteith, J., 1972. Solar radiation and productivity in tropical ecosystems. J. Appl. Ecol., 747–766.
Mu, S., Chen, Y., Li, J., et al., 2013a. Grassland dynamics in response to climate change and human activities in Inner Mongolia, China between 1985 and 2009. Rangeland J. 35, 315–329.
Mu, S., Zhou, S., Chen, Y., et al., 2013b. Assessing the impact of restoration-induced land conversion and management alternatives on net primary productivity in Inner Mongolian grassland, China. Global Planet. Change 108, 29–41.
Nemani, R.R., Keeling, C.D., Hashimoto, H., et al., 2003. Climate-driven increases in global terrestrial net primary production from 1982 to 1999. Science 300, 1560–1563.
Neupert, R.F., 1999. Population, nomadic pastoralism, and the environment in the Mongolian Plateau. Popul. Environ. 20, 413–441.
Piao, S., Fang, J., Zhou, L., et al., 2007. Changes in biomass carbon stocks in China's grasslands between 1982 and 1999. Global Biogeochem. Cycles 21, GB2002.
Piao, S., Fang, J., Zhou, L., et al., 2005. Changes in vegetation net primary productivity from 1982 to 1999 in China. Global Biogeochem. Cycles 19, GB2027.
Potter, C.S., Randerson, J.T., Field, C.B., et al., 1993. Terrestrial ecosystem production: a process model based on global satellite and surface data. Global Biogeochem. Cycles 7, 811–841.
Prince, S.D., 1991. A model of regional primary production for use with coarse resolution satellite data. Int. J. Remote Sens. 12, 1313–1330.
Rahman, A.F., Sims, D.A., Cordova, V.D., et al., 2005. Potential of MODIS EVI and surface temperature for directly estimating per-pixel ecosystem C fluxes. Geophys. Res. Lett. 32, L19404.
Running, S., Thornton, P., Nemani, R., et al., 2000. Global terrestrial gross and net primary productivity from the earth observing system. In: Sala, O., Jackson, R., Mooney, H. (Eds.), Methods in Ecosystem Science. Springer, New York, pp. 44–57.
Saxton, K.E., Rawls, W.J., Romberger, J.S., et al., 1986. Estimating generalized soil-water characteristics from texture. Soil Sci. Soc. Am. J. 50, 1031–1036.
Scurlock, J.M.O., Cramer, W., Olson, R.J., et al., 1999. Terrestrial NPP: toward a consistent data set for global model evaluation. Ecol. Appl. 9, 913–919.
Sims, D.A., Luo, H., Hastings, S., et al., 2006a. Parallel adjustments in vegetation greenness and ecosystem CO_2 exchange in response to drought in a Southern California chaparral ecosystem. Remote Sens. Environ. 103, 289–303.
Sims, D.A., Rahman, A.F., Cordova, V.D., et al., 2006b. On the use of MODIS EVI to assess gross primary productivity of North American ecosystems. J. Geophys. Res.: Biogeosci. 111, G04015.
Sims, D.A., Rahman, A.F., Cordova, V.D., et al., 2008. A new model of gross primary productivity for North American ecosystems based solely on the enhanced vegetation index and land surface temperature from MODIS. Remote Sens. Environ. 112, 1633–1646.
Thomey, M.L., Collins, S.L., Vargas, R., et al., 2011. Effect of precipitation variability on net primary production and soil respiration in a Chihuahuan Desert grassland. Global Change Biol. 17, 1505–1515.
Wang, J., Brown, D., Chen, J., 2013. Drivers of the dynamics in net primary productivity across ecological zones on the Mongolian Plateau. Landscape Ecol. 28, 725–739.
Wu, C., Chen, J.M., 2012. The use of precipitation intensity in estimating gross primary production in four northern grasslands. J. Arid Environ. 82, 11–18.
Wu, C., Han, X., Ni, J., et al., 2010a. Estimation of gross primary production in wheat from *in situ* measurements. Int. J. Appl. Earth Obs. Geoinf. 12, 183–189.
Wu, C., Munger, J.W., Niu, Z., et al., 2010b. Comparison of multiple models for estimating gross primary production using MODIS and eddy covariance data in Harvard Forest. Remote Sens. Environ. 114, 2925–2939.
Xiao, X., Hollinger, D., Aber, J., et al., 2004a. Satellite-based modeling of gross primary production in an evergreen needleleaf forest. Remote Sens. Environ. 89, 519–534.
Xiao, X., Zhang, Q., Braswell, B., et al., 2004b. Modeling gross primary production of temperate deciduous broadleaf forest using satellite images and climate data. Remote Sens. Environ. 91, 256–270.
Xiao, X., Zhang, Q., Hollinger, D., et al., 2005a. Modeling gross primary production of an evergreen needleleaf forest using MODIS and climate data. Ecol. Appl. 15, 954–969.
Xiao, X., Zhang, Q., Saleska, S., et al., 2005b. Satellite-based modeling of gross primary production in a seasonally moist tropical evergreen forest. Remote Sens. Environ. 94, 105–122.
Xie, Y., Sha, Z., Yu, M., et al., 2009. A comparison of two models with Landsat data for estimating above-ground grassland biomass in Inner Mongolia, China. Ecol. Modell. 220, 1810–1818.
Yu, D., Shao, H., Shi, P., et al., 2009a. How does the conversion of land cover to urban use affect net primary productivity? A case study in Shenzhen City, China. Agric. Forest Meteorol. 149, 2054–2060.
Yu, D., Shi, P., Shao, H., et al., 2009b. Modelling net primary productivity of terrestrial ecosystems in East Asia based on an improved CASA ecosystem model. Int. J. Remote Sens. 30, 4851–4866.